Vortex Line Ordering in the Driven Three-Dimensional Vortex Glass

Ajay Kumar Ghosh,[1,2] Peter Olsson,[1] and S. Teitel[3]

[1]*Department of Physics, Umeå University, 901 87 Umeå, Sweden*
[2]*Department of Physics, Jadavpur University, Kolkata 700032, India*
[3]*Department of Physics and Astronomy, University of Rochester, Rochester, New York 14627, USA*
(Received 9 March 2006; published 27 December 2006)

Resistively shunted junction dynamics is applied to the three-dimensional uniformly frustrated *XY* model with randomly perturbed couplings, as a model for driven steady states in a type-II superconductor with quenched point pinning. For a disorder strength p strong enough to produce a vortex glass in equilibrium, we map the phase diagram as a function of temperature T and uniform driving current I. Using finite size analysis and averaging over many realizations of quenched randomness we find a first-order melting $T_m(I)$ from a vortex line smectic to an anisotropic liquid.

PACS numbers: 74.25.Dw, 64.60.−i, 74.25.Qt, 74.40.+k

Ordering and phase transitions in driven steady states far from equilibrium remain topics of considerable general interest. In particular, the spatial ordering of driven vortex lines in a type-II superconductor with random point pinning has received considerable theoretical [1–4] and experimental [5] attention. Originally, Koshelev and Vinokur proposed [1] that a moving steady state would average over quenched randomness, and that a system which was disordered in equilibrium could reform into an ordered vortex lattice when driven. Later, Giamarchi and Le Doussal [2] argued that this state would be a "moving Bragg glass," with algebraically decaying translational correlations both parallel and transverse to the driving force. Balents, Marchetti, and Radzihovsky [3] then argued that the moving Bragg glass would be unstable to dislocations which decouple the planes of vortex lines moving parallel to the drive, resulting in a smectic ordering. Other theoretical works [4] have supported one or more of these scenarios.

While numerous simulations have studied this problem for point vortices in two dimensions [6], few works have treated three-dimensional (3D) vortex lines at finite temperature [7–10]. We present here the first 3D simulations to include both a systematic study of finite size effects as well as averaging over many realizations of the quenched randomness [11]. Such considerations are necessary for an unambiguous determination of ordering in driven steady states. We map the phase diagram as a function of temperature T and driving current I for the strongly random case, and study the nature of ordering just below and above the melting transition $T_m(I)$.

Following Refs. [8–10] we use the 3D *XY* model [12] with resistively shunted junction (RSJ) dynamics [13] to model our system. The Hamiltonian is given by

$$\mathcal{H}\left[\theta(\mathbf{r}_i)\right] = -\sum_{i\mu} J_{i\mu} \cos[\theta(\mathbf{r}_i) - \theta(\mathbf{r}_i + \hat{\mu}) - A_{i\mu}], \quad (1)$$

where $\theta(\mathbf{r}_i)$ is the phase of the superconducting wave function on site $\mathbf{r}_i$ of a cubic $L_x \times L_y \times L_z$ grid of sites with bonds in directions $\mu = x, y, z$. The circulation of $A_{i\mu}$

around any plaquette of the grid is fixed and equal to $2\pi f$ with f the density of applied magnetic flux quanta through that plaquette. We use a uniform value $f = 1/12$ oriented in the $\hat{z}$ direction. The resulting field induced vortex line density, also equal to f, forms a vortex lattice in the equilibrium ground state of the pure (disorder-free) system, with basis vectors $\mathbf{a}_1 = 4\hat{y}$ and $\mathbf{a}_2 = 3\hat{x} + 2\hat{y}$. To model quenched point randomness we use couplings [14] $J_{i\mu} = J_\mu(1 + p\epsilon_{i\mu})$, where $\epsilon_{i\mu}$ are uncorrelated, uniformly distributed, random variables with $\langle \epsilon_{i\mu} \rangle = 0$, $\langle \epsilon_{i\mu}^2 \rangle = 1$. We use $J_\mu = J_\perp$ in the xy plane, and $J_z = J_\perp/40$ to enhance vortex line fluctuations along the $\hat{z}$ direction. The disorder strength is controlled by the parameter p. In our earlier work [14,15] we showed that above a critical p_c the vortex line lattice becomes unstable to a vortex glass at low temperatures in equilibrium. Here we consider the strongly random limit $p = 0.15 > p_c \approx 0.14$.

We use RSJ dynamics, with the equation of motion as in [9], however, with fluctuating twist boundary conditions [13] in *all* directions. We apply a uniform current $\mathbf{I} = I\hat{x}$, resulting in a force $\hat{z} \times \mathbf{I}$ on the vortex lines driving them in the $\hat{y}$ direction. We use a second order Runge-Kutta integration method with dimensionless time step [9] $\Delta t = 0.1$, and typically 2.6×10^6 time steps per simulation run, resulting in a net displacement of the vortex line center of mass of roughly 48 000 grid spacings in the ordered phase. Depending on system size, up to $3/4$ of these steps may be discarded for equilibration. When probing behavior at a specific point in the T-I plane, we usually take the pure system ground state as our initial configuration. For numerous test cases, however, we have started with a random initial state at high T and slowly cooled to the desired point. Except for a narrow region of hysteresis at the melting transition, we always find the same long time steady state for both initial conditions.

To determine the structural order of our system, we use the vortex structure function

$$S(\mathbf{k}) = \frac{1}{fL_xL_yL_z} \sum_{\mathbf{R},\mathbf{r}} e^{i\mathbf{k}\cdot\mathbf{r}} \langle n_z(\mathbf{R} + \mathbf{r})n_z(\mathbf{R})\rangle, \quad (2)$$

where $n_z(\mathbf{r})$ is the vortex line density in the $\hat{z}$ direction at position $\mathbf{r}$. We use $\langle \cdots \rangle$ to denote averages over simulation time and $[\cdots]$ to denote averages over independent realizations of quenched randomness (typically 40 realizations are used). We also consider the correlations

$$C(x, y, z) = \frac{1}{L_x L_y L_z} \sum_{\mathbf{k}} S(\mathbf{k}) e^{-i\mathbf{k}\cdot\mathbf{r}}, \qquad (3)$$

$$\tilde{C}(x, k_y, z) = \frac{1}{L_x L_z} \sum_{k_x k_z} S(\mathbf{k}) e^{-i(k_x x + k_z z)}. \qquad (4)$$

Using the appearance of sharp peaks in $S(\mathbf{k}_\perp, k_z = 0)$ to signal an ordered phase, in Fig. 1(a) we present the T-I phase diagram for a $24 \times 24 \times 16$ sized system for both the pure ($p = 0$) and random ($p = 0.15$) cases. We measure T in units of $J_\perp$, and I in units of $I_0 = 2eJ_\perp/\hbar$. Crossing the phase boundary at any value of the current we find a discrete jump in energy, suggesting a first-order melting transition $T_m(I)$. For the random case, our phase boundary is from a single random realization only and is determined by two separate methods: by cooling in T at fixed I from the disordered phase (solid line); by increasing and decreasing I at fixed T from within the ordered phase (dashed line). Assuming some hysteresis, as in a first-order transition, the two methods give reasonable agreement. At fixed T, the random system orders only for a finite current interval $I_{c1}(T) < I < I_{c2}(T)$. For the pure case, our $T_m(I)$ looks qualitatively similar to that found in Ref. [9] for the weakly random case $p < p_c$. The melting of the ordered phase upon increasing $I > I_{c2}$, which exists for both random and pure systems, is contrary to theoretical predictions [1–4]. Reference [9] suggested this to be a
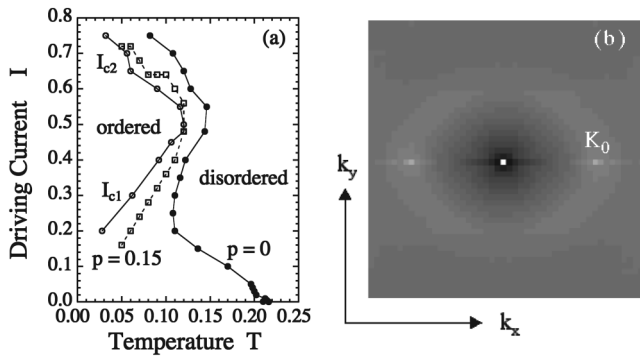
consequence of thermally excited vortex loops. We in fact find that the density of thermally excited loops is negligible everywhere in the ordered phase, but shows a finite jump to a noticeable amount as $T_m(I)$ is crossed; this jump is particularly large as I crosses $I_{c2}(T)$.

Consider first the disordered phase. Figure 1(b) shows an intensity plot of $\ln S(\mathbf{k}_\perp, k_z = 0)$ for a single realization of a random 48^3 system at $I = 0.48$, $T = 0.13$, just above the maximum in $T_m(I)$. Two relatively faint peaks, $S(\mathbf{K}_0)/S(0) \simeq 0.008$, lie off the origin along the k_x axis. Previous works [9,10] have interpreted such peaks as evidence for a smectic phase. However, as shown in Fig. 2(b), we find no significant increase of peak height $S(\mathbf{K}_0)$ with system size, thus indicating that this is an anisotropic liquid with only short ranged translational correlations.

Next consider the ordered phase. Figure 2(a) shows an intensity plot of $\ln S(\mathbf{k}_\perp, k_z = 0)$ for a single realization of a random 48^3 system at $I = 0.48$, $T = 0.09$, just below the maximum in $T_m(I)$. Now sharp peaks, $S_{\text{peak}}/S(0) \simeq 1$, lie along the k_x axis. In the *pure* system, the vortex lattice state has Bragg peaks at $\mathbf{K}_{10} = (2\pi/3)\hat{x}$ and $\mathbf{K}_{11} = (2\pi) \times (\hat{x}/6 + \hat{y}/4)$, as labeled in Fig. 2(a). In the random system a peak remains exactly at $\mathbf{K}_{10}$; a second peak is always found with $K_y = K_{11,y}$ but with $K_x - K_{11,x} = 0, \pm 2\pi/L_y$ depending on the particular random realization. We therefore generalize our notation to denote by $\mathbf{K}_{11}$ the exact location of this second peak, with the understanding that the value of $K_{11,x}$ may shift slightly between different random realizations. In Fig. 2(b) we plot the disorder averaged height of these peaks, $[S(\mathbf{K}_{10})]$ and $[S(\mathbf{K}_{11})]$, vs system volume, $V = L_x L_y L_z$, for several different system

FIG. 1. (a) Phase diagram as function of temperature T and uniform driving current $I\hat{x}$ (vortex lines move in the $\hat{y}$ direction). Solid symbols are for a pure system, $p = 0$. Open symbols are for a system with quenched point pinning, $p = 0.15$; $\bigcirc$ is phase boundary obtained by cooling T from the disordered phase at fixed I, while $\square$ is phase boundary obtained by increasing or decreasing I from the ordered phase at fixed T. Results are from a $24 \times 24 \times 16$ size system. (b) Intensity plot of $\ln S(\mathbf{k}_\perp, k_z = 0)$, for one particular random realization ($p = 0.15$), in disordered phase at $I = 0.48$, $T = 0.13$ for a $48 \times 48 \times 48$ size system; $\mathbf{k} = 0$ is at the center of the figure.
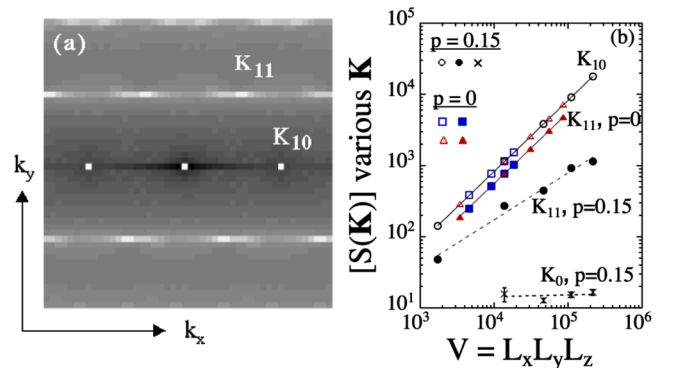

FIG. 2 (color online). (a) Intensity plot of $\ln S(\mathbf{k}_\perp, k_z = 0)$, for one particular random realization, in ordered phase at $I = 0.48$, $T = 0.09$ for a $L_x = L_y = L_z = 48$ size system; $\mathbf{k} = 0$ is at the center of the figure. (b) Scaling of disorder averaged peaks heights vs system volume $V = L_x L_y L_z$. For the ordered state of (a) we plot $[S(\mathbf{K}_{10})]$ and $[S(\mathbf{K}_{11})]$ for pure ($p = 0$) systems of size $24 \times 24 \times L$ (squares) and $L \times L \times 24$ (triangles), and for systems with quenched point pinning ($p = 0.15$) of size L^3, $L = 12, 24, 36, 48, 60$ (circles). We also plot $[S(\mathbf{K}_0)]$ for the $p = 0.15$ disordered state at $T = 0.13$ of Fig. 1(b) for systems of size L^3 with $L = 24, 36, 48, 60$ (crosses).

sizes, for both the pure and random cases. In both cases $[S(\mathbf{K}_{10})]$ scales linearly with V, indicating a sharp Bragg peak. This Bragg peak indicates that vortex lines are organized into specific yz planes with a periodic spacing of $3\hat{x}$ between planes. Ordering within and between planes is reflected in the scaling of $[S(\mathbf{K}_{11})]$. For the pure case, $S(\mathbf{K}_{11}) \sim V$, indicating the long range translational order of a moving vortex line lattice. For the random case, however, $[S(\mathbf{K}_{11})]$ grows less rapidly than V. The dashed line Fig. 2(b) represents a power law divergence of $[S(\mathbf{K}_{11})] \sim V^{2/3} \sim L^2$; however, if we discard the smallest point at $L = 12$, the exponent of a power law fit in L becomes 1.65. It is thus unclear from Fig. 2(b) whether our biggest size system has reached the asymptotically large L limit. The sublinear growth of $[S(\mathbf{K}_{11})]$ with V indicates that the system has less than long range translational order. However, it does not indicate which direction(s) are less ordered than others. For this we will consider the shape of the peak at $\mathbf{K}_{11}$ and the real space correlations of Eqs. (3) and (4).

The sharpness of the peak at $\mathbf{K}_{11}$ in the $\hat{k}_y$ direction suggests that vortex lines are periodically ordered along their direction of motion $\hat{y}$ within each yz plane. That this peak appears broad in the $\hat{k}_x$ direction suggests that the yz planes have only short range correlations between them. We thus refer to the yz planes containing the vortex lines as *smectic* planes. We now consider the real space correlations of Eqs. (3) and (4). Figure 3(a) shows an intensity plot of $C(x, y, z = 0)$ corresponding to $S(\mathbf{k})$ of Fig. 2(a). We clearly see the structure proposed above: vortices lie in periodically spaced yz planes with separation $3\hat{x}$; within a given plane, i.e., $x = 0$, vortices are periodic with separation $4\hat{y}$; at finite transverse separation, i.e., $|x| > 0$, the variation of $C(x, y, 0)$ with y decreases, until at large $|x|$ it is almost uniform in y, thus indicating short ranged correlations between the smectic planes. To quantify this,

we consider the correlation Eq. (4) evaluated at $k_y = K_{11,y}$ giving the periodicity within a given smectic plane. Since the slightly different values of $K_{11,x}$ for the different random realizations give rise to different complex phase shifts in $\tilde{C}(x, K_{11,y}, z = 0)$, we disorder average the absolute value. In Fig. 3(b) we plot $[|\tilde{C}(x, K_{11,y}, 0)|]/C_0$ vs x, for different system sizes L^3. We normalize by $C_0 \equiv [|\tilde{C}(0, K_{11,y}, 0)|]$ to better compare different system sizes. We see a clear exponential decay to zero; solid lines are fits to a periodic exponential giving correlation lengths in the range $\xi_x \sim 5$–6.5. In recent works [9,10] pictures similar to Fig. 2(a) were identified as a moving Bragg glass. However, the short range correlations of Fig. 3(b) clearly show our ordered phase to be a smectic rather than a Bragg glass.

Next we consider correlations parallel to the direction of motion $\hat{y}$, within a given smectic plane. Figure 4(a) shows $[C(0, y, 0)]$ vs y, for various system sizes, for the same $I = 0.48$, $T = 0.09$ as in Figs. 2 and 3. Since we found $\xi_x \sim 6$ is fairly small, we include also systems of size $36 \times L \times L$ in order to obtain larger values of L_y. Figure 4 suggests decay to a periodic oscillation, with only a small finite size effect when $y \sim L_y/2$. The large y limit can be described by the three envelop functions, $[C_{\max}(L_y)] \equiv \min_m[C(0, 4m, 0)]$, $[C_{\min}(L_y)] \equiv \max_m[C(0, 4m + 2, 0)]$, and $[C_{\mathrm{mid}}(L_y)] \equiv \max_m[C(0, 4m \pm 1, 0)]$, for m integer, which we plot vs L_y in Fig. 4(b). For long range translational order, these should converge to different constants as $L_y \to \infty$. For algebraic or short range order, these should all converge to the value $1/4$ characterizing a uniform vortex line density. We find that both exponential decay to long range order (red solid line) and an algebraic decay to $1/4$ (blue dashed line) give equally good fits. For long
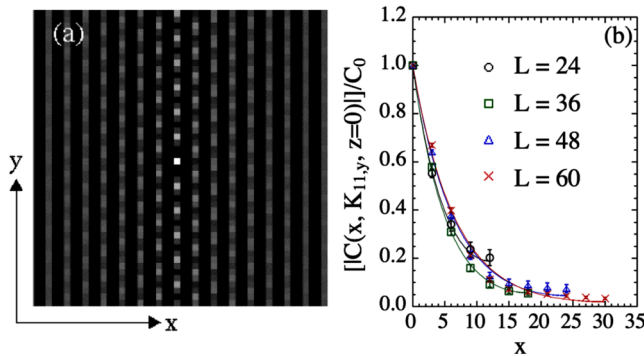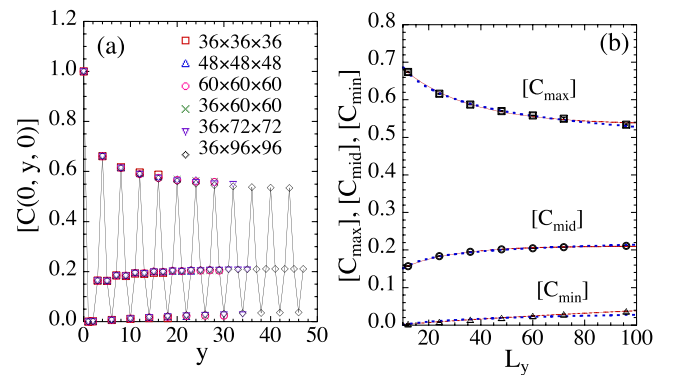

FIG. 3 (color online). (a) Intensity plot of real space correlation, $C(x, y, z = 0)$, for one particular random realization, in ordered phase at $I = 0.48$, $T = 0.09$, $p = 0.15$, for a $L_x = L_y = L_z = 48$ size system; $\mathbf{r} = 0$ is at the center of the figure. (b) Corresponding disorder averaged correlation, $[|\tilde{C}(x, K_{11,y}, z = 0)|]$ vs x for systems of size $L \times L \times L$.

FIG. 4 (color online). (a) Disorder averaged real space correlation, $[C(x = 0, y, z = 0)]$ vs y for various system sizes, in the ordered phase at $I = 0.48$, $T = 0.09$, $p = 0.15$. (b) Corresponding limiting values of maximum, middle, and minimum envelop of $[C(x = 0, y, z = 0)]$ (see text) vs L_y for various system sizes; the red solid line is a fit to an exponential decay to a constant, and the blue dashed line is a fit to an algebraic decay to $1/4$.
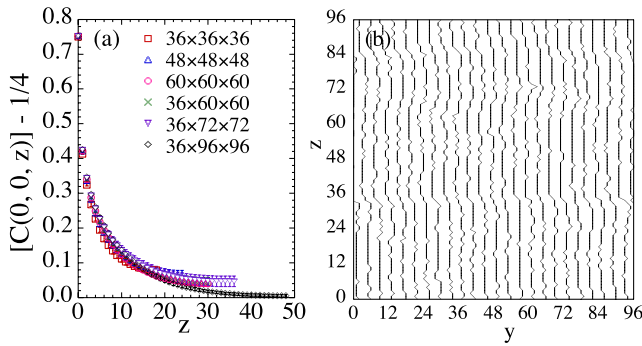
FIG. 5 (color online). (a) Disorder averaged real space correlation, $[C(x = 0, y = 0, z)] - 1/4$ vs z for various system sizes, in the ordered phase at $I = 0.48$, $T = 0.09$, $p = 0.15$. (b) Instantaneous vortex line configuration in a particular smectic plane of a particular random realization, in the ordered phase at the same parameters as (a), for a system of size $36 \times 96 \times 96$.

range order, the fit to $[C_{\max}]$ gives a decay length $\xi_y \sim 25$, while the algebraic fit to $[C_{\max}]$ gives a power law exponent of ~ 0.2.

Finally, we consider the correlations along $\hat{z}$, parallel to the applied magnetic field, within a given smectic plane. Figure 5(a) shows $[C(0, 0, z)] - 1/4$ vs z, for various system sizes, for the same $I = 0.48$, $T = 0.09$ as before. The subtracted value $1/4$ is the uniform vortex density in the smectic plane, in the absence of any ordering. For the largest system size $L_y = 96$ we find an exponential decay to zero with a decay length $\xi_z \sim 9$. Smaller sizes show a decay to a small finite constant that decreases with increasing L_y, consistent with our earlier observation in Fig. 2(b) that $[S(\mathbf{K}_{11})]$ has not yet reached the asymptotic large L limit for $L \lesssim 60$. In Fig. 5(b) we show an instantaneous configuration of vortex lines in a particular smectic plane. At fixed z, the lines appear periodically spaced along y, in agreement with Fig. 4. However, tracing any particular line along z, we see that it wanders an amount comparable to the interline spacing, consistent with the decay seen in Fig. 5(a). In some planes, such as the one shown in Fig. 5(b), lines can have a net tilt, by closing onto one of their neighbors under the periodic boundary condition along $\hat{z}$. Each such tilted plane must be compensated by another plane that tilts in the opposite direction, so that the net vorticity in the $\hat{y}$ direction vanishes. Looking at individual configurations, we find a strong relation between the correlations along $\hat{z}$ within a given smectic plane and the correlations along $\hat{x}$ between different smectic planes. When the lines in a smectic plane are tilted, as in Fig. 5(b), or otherwise have a transverse wandering comparable to the average spacing between lines, we find that this plane decouples from its neighbors, moving either diffusively with respect to its neighbors, or even with a slightly different average speed. Planes whose lines have small transverse wanderings, remain strongly correlated

with their neighbors. It is necessary to have only a few such decoupled smectic planes in order to have short range average correlations along $\hat{x}$, as in Fig. 3(b).

Our analysis of the ordered phase has been for a point just below the peak in the first-order melting curve $T_m(I)$. Establishing the nature of correlations throughout the ordered phase would require similar finite-size, random-realization-averaged analyses elsewhere in this region. Our preliminary investigations suggest that as either T or I is decreased, finite correlation lengths grow and become too large to make such studies feasible at present. We thus cannot rule out the possibility of a more ordered moving Bragg glass phase at lower temperatures.

[1] A. E. Koshelev and V. M. Vinokur, Phys. Rev. Lett. **73**, 3580 (1994).

[2] T. Giamarchi and P. Le Doussal, Phys. Rev. Lett. **76**, 3408 (1996).

[3] L. Balents, M. C. Marchetti, and L. Radzihovsky, Phys. Rev. Lett. **78**, 751 (1997); Phys. Rev. B **57**, 7705 (1998).

[4] S. Scheidl and V. M. Vinokur, Phys. Rev. E **57**, 2574 (1998); P. Le Doussal and T. Giamarchi, Phys. Rev. B **57**, 11 356 (1998).

[5] S. Bhattacharya and M. J. Higgins, Phys. Rev. Lett. **70**, 2617 (1993); M. Marchevsky *et al.*, Phys. Rev. Lett. **78**, 531 (1997); F. Pardo *et al.*, Nature (London) **396**, 348 (1998); A. M. Troyanovski *et al.*, Nature (London) **399**, 665 (1999); Z. L. Xiao *et al.*, Phys. Rev. Lett. **85**, 3265 (2000); Y. Togawa *et al.*, Phys. Rev. Lett. **85**, 3716 (2000); A. Maeda *et al.*, Phys. Rev. B **65**, 054506 (2002).

[6] H. Fangohr *et al.*, Phys. Rev. B **64**, 064505 (2001), and references therein.

[7] A. van Otterlo *et al.*, Phys. Rev. Lett. **84**, 2493 (2000); C. J. Olson, C. Reichhardt, and V. M. Vinokur, Phys. Rev. B **64**, 140502(R) (2001); T. J. Bullard *et al.*, cond-mat/0511509.

[8] D. Domínguez *et al.*, Phys. Rev. Lett. **78**, 2644 (1997).

[9] Q.-H. Chen and X. Hu, Phys. Rev. Lett. **90**, 117005 (2003).

[10] Q.-M. Nie *et al.*, Int. J. Mod. Phys. B **18**, 2476 (2004).

[11] Reference [8] does finite size scaling, but no disorder averaging. The high vortex density $f = 1/6$ used in this work may also enhance grid effects as compared to later works.

[12] T. Chen and S. Teitel, Phys. Rev. B **55**, 11 766 (1997).

[13] B. J. Kim *et al.*, Phys. Rev. B **59**, 11 506 (1999); D. Domínguez, Phys. Rev. Lett. **82**, 181 (1999).

[14] P. Olsson and S. Teitel, Phys. Rev. Lett. **87**, 137001 (2001).

[15] P. Olsson, Phys. Rev. Lett. **91**, 077002 (2003); Phys. Rev. B **72**, 144525 (2005).